molecular pharmaceutics

Article

Cite This: Mol. Pharmaceutics XXXX, XXX, XXX−XXX

Short Drug−Light Intervals Improve Liposomal Chemophototherapy in Mice Bearing MIA PaCa-2 Xenografts

Dandan Luo, Kevin A. Carter, Jumin Geng, Xuedan He, and Jonathan F. Lovell*

Department of Biomedical Engineering, University at Buffalo, State University of New York, Buffalo, New York 14260, United States

Supporting Information

ABSTRACT: Chemophototherapy (CPT) is an emerging tumor treatment that combines phototherapy and chemotherapy. Long-circulating (LC) liposomes can stably incorporate 2 mol % porphyrin-phospholipid (PoP) in the bilayer and load doxorubicin (Dox) to generate LC-Dox-PoP liposomes, for single-agent CPT. Following intravenous administration to mice, LC-Dox-PoP liposomes (2 mg/kg Dox) circulated with similar blood concentration ranges produced by a typical human clinical dose of DOXIL (50 mg/m^2 Dox). This dosing approach aims to achieve physiologically relevant Dox and PoP concentrations as well as CPT vascular responses in mice bearing subcutaneous human pancreatic MIA PaCa-2 xenografts. Phototreatment with 2 mg/kg LC-Dox-PoP induced vascular permeabilization, leading to a 12.5-fold increase in Dox tumor influx estimated by a pharmacokinetic model, based on experimental data. Shorter drug−light intervals (0.5−3 h) led to greater tumoral drug deposition and improved treatment outcomes, compared to longer drug−light intervals. At 2 mg/kg Dox, CPT with LC-Dox-PoP liposomes induced tumor regression and growth inhibition, whereas chemotherapy using several other formulations of Dox did not. LC-Dox-PoP liposomes were well tolerated at the 2 mg/kg dose.

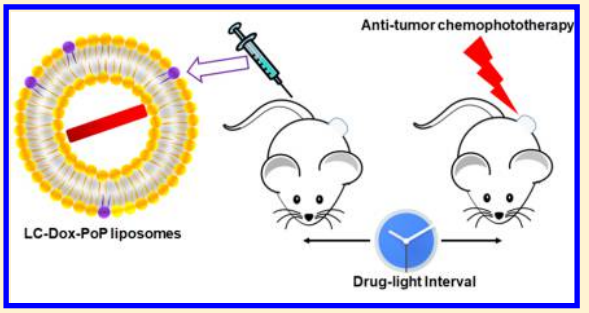

KEYWORDS: *chemophototherapy, photodynamic therapy, drug−light interval, chemotherapy, liposomes, doxorubicin*

INTRODUCTION

Chemophototherapy (CPT) is an emerging tumor treatment that aims to synergistically combine chemotherapy and phototherapy.[1,2] Numerous approaches have been described to load various drugs into novel nanocarriers and trigger their release using light.[3−10] Porphyrin-phospholipid (PoP) can stably be incorporated into the bilayer of liposomes and, when subjected to near-infrared (NIR) light, trigger the release of diverse types of encapsulated cargos.[11−16] We recently described the composition of a long-circulating, photoactivatable, doxorubicin (Dox) encapsulated PoP liposome (LC-Dox-PoP liposome) that has a similar composition to FDA-approved DOXIL, but contains 2 mol % PoP in the bilayer.[17]

In this study, we use LC-Dox-PoP to examine the impact of the drug−light interval (DLI) for single-agent CPT. We previously demonstrated that when LC-Dox-PoP liposomes (5−10 mg/kg Dox) are irradiated with near-infrared light (NIR) up to 1 h after intravenous administration (i.e., a 1 h DLI), up to 7-fold increase in drug accumulation is observed in the tumor 24 h after laser treatment, due to PDT induced vascular permeabilization.[14,17,18] Other groups have also demonstrated that PDT can augment nanoparticle accumulation with two agent systems (i.e., a separate photosensitizer and nanoparticle).[19−22]

In photodynamic therapy (PDT), the duration between photosensitizer administration and light administration impacts antitumor outcomes, so the DLI is an important consideration.[23,24] Some photosensitizers such as Photofrin are administered days prior to light treatment, to allow for good deposition of the photosensitizer to the target site, while also improving the ratio of photosensitizer in the tumor compared to the skin.[25] However, other photosensitizers such as temoporfin,[23,24,26] hypericin,[27] and mono-L-aspartyl chlorin e6[28] can use shorter DLIs, relying on vascular PDT damage rather than direct tumor cell kill. Several studies have suggested that the amount of photosensitizer in the plasma at the time of irradiation influences therapeutic outcomes.[23,24,27,28] To our knowledge, the impact of DLI has not yet been addressed with single-agent CPT.

METHODS AND MATERIALS

Liposome Preparation. The porphyrin-phospholipid (PoP) used was *sn*-1-palmitoyl, *sn*-2-pyropheophorbide phosphatidylcholine and was synthesized as previously reported.[14] 1,2-Distearoyl-*sn*-glycero-3-phosphocholine (DSPC; #LP-R4-076), cholesterol (#CH-0355), 1,2-distearoyl-phosphatidylethanolamine-methyl-polyethylene glycol conjugate-2000 (DSPE-2000-PEG; #LP-R4-039) were from Corden Pharma. Long-circulating PoP liposomes [DSPC:PoP:cholesterol:DSPE-2000-

Special Issue: New Directions for Drug Delivery in Cancer Therapy

Received: January 17, 2018
Revised: March 9, 2018
Accepted: March 23, 2018

DOI: 10.1021/acs.molpharmaceut.8b00052
Mol. Pharmaceutics XXXX, XXX, XXX−XXX

PEG] [53:2:40:5, molar ratio] were prepared by a modified hot ethanol injection method followed by high pressure extrusion as previously described.[17,29] To generate 10 mL of PoP liposomes (20 mg/mL total lipids), 114.1 mg of DSPC, 42.2 mg of cholesterol and 38.2 mg of DSPE-2000-PEG, and 5.52 mg of PoP were fully dissolved in 2 mL of hot ethanol, followed by direct injection into 8 mL of 250 mM ammonium sulfate (pH 5.5) buffer at 60 °C. Lipid solution was passed 10 times through sequentially stacked 0.2, 0.1, and 0.08 μm polycarbonate membranes using a 10 mL LIPEX nitrogen pressurized extruder (Northern Lipids) at 60 °C. To remove free ammonium sulfate, liposome solutions were then dialyzed with buffer containing 10% sucrose and 10 mM histidine (pH 6.5) with three buffer exchanges. Doxorubicin (LC Laboratories #D-4000) was actively loaded by adding a 20 mg/mL Dox solution to the liposomes at a drug to lipid molar ratio of 1:6 and incubating at 60 °C for 1 h. Drug loading efficacy was generally over 95% and size ~90 nm with good homogeneity.[17] Preparation of DOXIL-like liposomes [HSPC:cholesterol:DSPE-2000-PEG] [56:39:5, molar ratio][30](Dox to lipid molar ratio 1:6) was the same as that of PoP liposomes described above. Likewise, preparation of Myocet-like liposomes [egg PC:cholesterol] [55:45, molar ratio] (Dox to lipid molar ratio 1:8) was the same as that of LC-Dox-PoP liposomes except the active loading buffer was sodium citrate (300 mM, pH 4.0).[30]

Pharmacokinetics. Animal studies were approved by the Institutional Animal Care and Use Committees of University at Buffalo. For pharmacokinetics (PK) studies, BALB/c mice (female, 18−20 g, Charles River) were intravenously injected via tail vein with LC-Dox-PoP liposomes at 1, 2, or 5 mg/kg (n = 3 mice per group). Small blood volumes were sampled from either saphenous, submandibular, or retroorbital locations at 0.5, 2, 4, 9, 24, and 48 h post drug administration. Blood was collected with a serum capillary tube (Sarstedt Microvette CB 300 Z) centrifuged at 1500g for 15 min, and diluted in extraction buffer (0.075 N HCL, 90% isopropanol). Samples were then stored at −20 °C overnight followed by centrifugation at 10000g for 15 min. Supernatants were collected and analyzed by fluorescence (480 nm excitation, 590 nm emission) in a 96 well plate reader, and concentration was determined from a standard curve. Noncompartmental analysis was performed in Phoenix WinNonlin (version 7.0, Pharsight) with linear-log trapezoidal method.

A two-compartment model was used to describe the PK of liposomal doxorubicin (Figure 1A). The PK parameters were estimated, as shown in Table 1. Equations of PK model and an initial conditions (IC) describing the model are as follows.

The PK of LC-Dox-PoP liposomes in serum was described as

$$V_p \frac{dC_p}{dt} = -Q \cdot C_p + Q \cdot C_t - CL \cdot C_p \quad IC = dose \tag{1}$$

$$V_t \frac{dC_t}{dt} = Q \cdot C_p - Q \cdot C_t \quad IC = 0 \tag{2}$$

where C_p and C_t are the concentrations of Dox in serum (central compartment V_p) and tissue (second compartment V_t), CL is clearance from the central compartment, and Q is distribution to second compartment. The PK of liposomal Dox in tumor prior to laser treatment was described as

$$\frac{dX_{tu}}{dt} = k_1 \cdot X_p - k_2 \cdot X_{tu} \quad IC = 0 \tag{3}$$

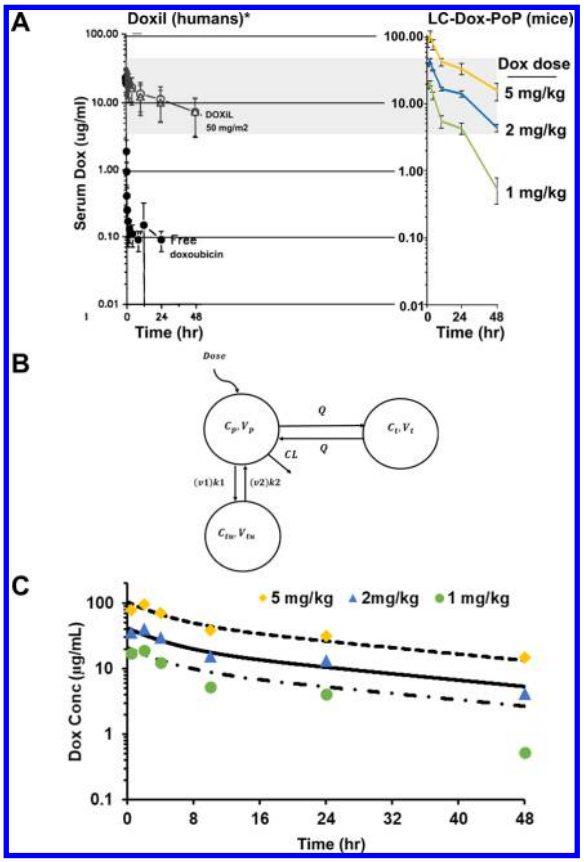

Figure 1. Pharmacokinetics of LC-Dox-PoP liposomes. Mice were administered LC-Dox-PoP liposomes via tail vein (1, 2, or 5 mg/kg Dox), and serum Dox concentrations were measured. (A) Human Doxil data (*adapted from ref 38) compared to LC-Dox-PoP. The gray highlighting shows the 2 mg/kg LC-Dox-PoP blood concentration range. Data represent mean ± SD for n = 3. (B) 2-Compartment plasma PK model and tumoral drug disposition model. (C) Observed data and plasma PK model of LC-Dox-PoP liposomes. Each line is from model fitting, and observed data are shown as symbols.

After the tumors were treated with laser, the PK of liposomal Dox in tumor was described as

$$\frac{dX_{tu}}{dt} = v_1 \cdot k_1 \cdot X_p - v_2 \cdot k_2 \cdot X_{tu} \quad IC = 0 \tag{4}$$

where X_{tu} represents the mass of Dox in tumor, X_p is the mass of Dox in serum, k_1 is the tumor influx rate constant of Dox without CPT laser treatment, and v_1 is the vascular permeabilization factor on k_1 due to the laser treatment. k_2 is the tumor efflux rate constant of Dox without laser, and v_2 is the vascular permeabilization factor on k_2 due to the laser treatment. Since the final time point of analysis was 24 h following laser treatment, tumor efflux parameter could not be estimated, so a constant efflux rate constant from other work with LC-Dox-PoP was assumed.[31] The approach of modulating baseline tumor influx/efflux rate using a coefficient has been used previously to describe the improved liposome uptake in tumor models.[32]

Tumoral Drug Uptake. Female athymic nude mice (5 weeks old, Jackson Laboratories, #007850) were inoculated with 5 × 10^6 MIA Paca-2 cells contralaterally on both flanks. When tumor sizes reached 6−8 mm, mice were randomly grouped into 6 groups (n = 4 mice per group). All mice were

DOI: 10.1021/acs.molpharmaceut.8b00052
Mol. Pharmaceutics XXXX, XXX, XXX−XXX

Table 1. Noncompartmental Analysis of PK of LC-Dox-PoP Liposomes

dose	$T_{(1/2)}$ (h)	C_{max} (μg/mL)	$AUC_{(0-t)}$ (μg/mL·h)	$AUC_{(0-inf)}$ (μg/mL·h)	CL (mL/h)	V_{SS} (mL)
1 mg/kg	9.8	19.1	223	231	0.087	1.26
2 mg/kg	16.6	40.9	667	768	0.052	1.23
5 mg/kg	25.0	95.2	1677	2207	0.045	1.52
Doxil 25 mg/m^2 [a]	45.2[b]	12.6		609	80	4100
Doxil 50 mg/m^2 [a]	45.9[b]	21.2		902	90	5900

[a]Human Doxil PK data was reproduced from ref 38. [b]Second $T_{(1/2)}$.

intravenously injected via tail vein with LC-Dox-PoP liposomes (2 mg/kg Dox). Tumors on one flank of the mice were irradiated (150 mW/cm^2 for 27.7 min, 250 J/cm^2, with a 665 nm laser diode) 0.5, 3, 6, 9, or 12 h after drug administration. Tumors on the other flank of the mice were not irradiated. All mice were sacrificed 24 h post drug administration. Tumors and key organs were collected and Dox and PoP were determined as previously described.[17] Briefly, tumors and key organs were washed in PBS. ~100 mg of tissue was weighed and homogenized in 450 μL of nuclear lysis buffer [250 mM sucrose, 5 mM Tris-HCl, 1 mM $MgSO_4$,1 mM $CaCl_2$ (pH 7.6)] with a homogenizer (Bullet Blender Storm). 100 μL of homogenate was extracted with 900 μL of 0.075 N HCI 90% isopropanol and storage at −20 °C overnight. Samples were removed and centrifuged at 10000g for 15 min. Supernatants were collected, and the concentrations of Dox (480 nm excitation, 590 nm emission) and PoP (420 nm excitation, 670 nm emission) were determined fluorometrically based on a standard curve.

Tumor Growth Inhibition. When subcutaneous MIA PaCa-2 tumor diameters reached 5−8 mm, mice were randomly grouped into 10 groups, 6 mice per group: (1) LC-Dox-PoP liposomes with 1 h DLI; (2) LC-Dox-PoP liposomes with 3 h DLI; (3) LC-Dox-PoP liposomes with 6 h DLI; (4) LC-Dox-PoP liposomes with 24 h DLI; (5) untreated control; (6) empty PoP liposomes with 3 h DLI; (7) LC-Dox-PoP liposomes without laser treatment; (8) Doxil-like liposomal Dox + 3 h DLI; (9) Myocet-like liposomal Dox; and (10) free Dox. All treatments that contained Dox were dosed at 2 mg/kg Dox. 200 μL of liposomal Dox (2 mg/kg Dox, 0.29 mg/kg PoP) or equivalent empty PoP liposomes (0.29 mg/kg PoP) were intravenously injected via tail vein. Laser irradiation was initiated with the indicated drug−light intervals (150 mW/cm^2 for 44.4 min, 400 J/cm^2). During this period, mice were anesthetized and placed on a heating pad to maintain body temperature around 35 °C. Tumor volumes were calculated using the ellipsoid formula, volume $= \pi \cdot L \cdot \frac{W^2}{6}$, where L and W are the length and width of the tumor, respectively. Body weights of the mice were monitored for 3 weeks. Mice were sacrificed when tumor volumes exceeded 10 times the initial volumes or at the end of this study (80 days). For the calculation of the delay for tumor doubling time, 80 days was used for the mice that were cured.

Data Analysis. GraphPad Prism (Version 5.01) software was used for data analysis. Difference was considered significant at $p < 0.05$ ($^*p < 0.05$, $^{**}p < 0.01$, $^{***}p < 0.001$). The ADAPT 5 software was used for all data fitting and simulation.[33] The maximum likelihood method was used for fitting the data. Replicate data at each time point from animals in each experiment were naive-pooled, and plasma PK and tumoral PK for both laser treated and non laser treated were fitted simultaneously. Visual inspection of the fitting curves, objection function values such as Akaike information criterion (AIC), improved likelihood, and precision (CV %) of the estimated parameters were used to evaluate the goodness of fit and model selection. The following variance model was used for the model fitting:

$$V_i = V(\theta, \sigma, t) = [(\sigma_1 + \sigma_2 \cdot Y(\theta, t_i)]^2 \quad (5)$$

where $V(\theta, \sigma, t)$ is the variance for the ith point, θ represents the estimated structural parameters, $Y(\theta, t_i)$ is the ith model-predicted value, and σ_1 and σ_2 are the variance parameters that were estimated.

Toxicity Study. ICR mice were intravenously administered LC-Dox-PoP liposomes (2 mg/kg Dox) or PBS ($n = 5$ for each group). Two weeks later, blood was collected. Complete blood count and serum chemistry profile were analyzed with VetScan HM5. Blood count parameters and their units include white blood cell count (WBC, 10^9/L), lymphocytes (LYM, 10^9/L), monocyte (MON, 10^9/L), neutrophil(NEU, 10^9/L), eosinophil (EOS, 10^9/L), basophils (BAS, 10^9/L), lymphocyte percentage (LY, %), monocyte percentage (MO, %), neutrophil percentage (%), eosinophil percentage (%), basophil percentage (BA, %), red blood cell count (RB, C%), hemoglobin (HGB, 10^{12}/L), hematocrit (HCT, %), mean corpuscular volume (MCV, fL), mean corpuscular hemoglobin (MCH), mean corpuscular hemoglobin count (MCHC g/dL), red blood cell distribution width (RDWc, %), platelet count(PLT, 10^9/L), platelet percentage (PCT, %), mean platelet volume (MPV, fL), and platelet distribution width (PDWc, %). Serum chemistry parameters include albumin (ALB, g/dL), alkaline phosphatase (ALKP, U/L), alanine transaminase (ALT, U/L), amylase (AMYL, U/L), calcium (Ca, mg/dL), cholesterol (CHOL, mg/dL), creatinine (CREA, mg/dL), glucose (GLU, mg/dL), phosphorus (PHOS, mg/dL), total bilirubin (TBIL, mg/dL), total protein (TP, g/dL), blood urea nitrogen (BUN, mg/dL), and globulin (GLOB, g/dL). Histology was performed by standard procedure. Briefly, key organs (heart, liver, spleen, lung, and kidney) were collected and fixed in 10% formalin for 24 h followed by immersion in 70% ethanol for 24 h. Formalin-fixed paraffin sections were cut at 4 μm. Slides were dewaxed through xylenes and graded alcohols, transferred to water for 3 min, hematoxylin for 3 min, water for 3 min, 1% acid alcohol for 1 min, water for 3 min, 0.2% ammonium hydroxide for 3 min, water for 4 min, 95% ethanol for 3 min, Eosin for 30 s, then dehydrated through graded alcohols, cleared, mounted and coverslipped with xylene mount.

RESULTS AND DISCUSSION

Physiologically Relevant LC-Dox-PoP Liposome Dosing. The pharmacokinetics (PK) of LC-Dox-PoP liposomes were evaluated in mice at Dox doses of 1, 2, or 5 mg/kg with intravenous injection. The composition of LC-Dox-PoP liposome is similar to that of Doxil,[17] an FDA-approved, PEGylated, long circulating formulation of Dox. Doxil is

DOI: 10.1021/acs.molpharmaceut.8b00052
Mol. Pharmaceutics XXXX, XXX, XXX−XXX

typically dosed at 50 mg/m^2 every 4 weeks in metastatic ovarian and breast cancer patients.[34,35] For a 60 kg patient, this works out to approximately 1.35 mg/kg.[36] The blood concentration of Doxil in humans at 50 mg/m^2 (C_{max} 21.2 μg/mL vs 40.3 μg/mL, Table 1, gray box in Figure 1A[37,38]) was comparable to the observed Dox blood concentration with 2 mg/kg LC-Dox-PoP in mice. Since the blood concentration of photosensitizer is a critical factor in a vascular PDT response, it is possible to directly study the vascular response of LC-Dox-PoP liposomes in the range of clinically relevant concentrations in mice. In other words, the plasma concentration of PoP in human at 50 mg/m^2 LC-Dox-PoP liposomes would be in a reasonably similar range to that in mice at 2 mg/kg dosage.

The PK of LC-Dox-PoP liposomes was dose-disproportional, with higher clearance at 1 mg/kg Dox compared to 2 mg/kg or 5 mg/kg (0.087 mg/L vs 0.052 mL/h and 0.045 mL/h, Table 1). This is likely due to saturation of the reticuloendothelial system at a higher dose.[39] The half-life of LC-Dox-PoP liposomes increased from 9.8 h at 1 mg/kg to 16.6 h at 2 mg/kg. A 2-compartment model adequately described the PK of LC-Dox-PoP liposomes (Figure 1B, Table 2). The model may have some overestimation of Dox concentration at the 1 mg/kg dose due to the faster observed clearance at lower drug dose. The estimated clearance 0.051 mL/h from the 2-compartment model is close to the results from the NCA analysis (Table 1, Table 2). Overall, the PK model matched well with experimental data (Figure 1C).

Table 2. Two-Compartment Model Parameter Estimates

parameter	definition	estimate	CV %
CL (mL/h)	clearance	0.048	7.5
V_p (mL)	vol of central compartment	0.96	6.9
V_t (mL)	vol of second compartment	0.6	28.3
Q (mL/h)	distribution to second compartment	0.073	38.5

Drug Accumulation with Various Drug–Light Intervals. Using a 2 mg/kg intravenous dose of LC-Dox-PoP liposomes, tumor-bearing mice were irradiated on the tumor with a 0.5, 3, 6, 9, or 12 h DLI following drug administration. Dox concentration in the tumor was assessed 24 h after drug injection. With a 0.5 h DLI, tumoral Dox concentration increased by 10.9-fold compared to nonirradiated tumors. Shorter DLIs led to higher amounts of Dox accumulation 24 h post drug administration. Despite this trend, laser-treated tumoral Dox concentrations between the 0.5 h DLI and DLIs of 3, 6, and 9 h were not statistically different (one-way ANOVA and Tukey's test). However, tumoral Dox concentration with a 0.5 h DLI was significantly greater than with a 12 h DLI ($*p < 0.05$) and no laser control ($**p < 0.01$). The enhanced Dox uptake with shorter DLIs is likely due to the higher blood concentration of LC-Dox-PoP at the time of irradiation, which consequently leads to greater drug accumulation into permeabilized vasculature. A pharmacokinetic model with a first order tumoral Dox influx rate k_1 and efflux rate k_2 was developed to account for the tumoral Dox concentration after laser treatment, assuming that the tumoral influx rate and efflux rates remain the same for different DLIs (Figure 2A, Table 3). The model adequately described the tumoral Dox concentration 24 h post dosing for most DLIs except for the 0.5 h DLI (Figure 2B). The underestimation of tumoral Dox concentration at DLI 0.5 h may be due to greater initial tumor influx rate increase than the estimated 12.5-fold increase (Table 3).

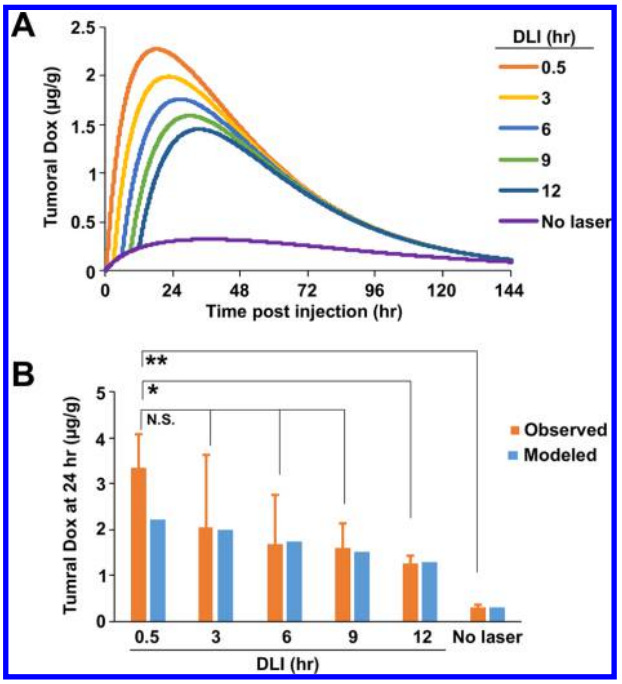

Figure 2. Shorter DLIs led to greater tumoral Dox exposure in MIA PaCa-2 xenografts. (A) PK modeling of tumoral doxorubicin concentration kinetics after phototreatment with varying DLIs. (B) Observed and modeled tumoral Dox accumulation 24 h after drug administration (2 mg/kg LC-Dox-PoP) with indicated DLI. Experimental data are presented as mean ± SD for $n = 4$. Significance relative to the 0.5 h DLI group is based on one-way ANOVA followed by post hoc Tukey's test: $*p < 0.5$; $**p < 0.01$; N.S., not significant.

Table 3. Tumoral PK Parameters

parameter	definition	estimate	CV %
k_1 (h^{-1})	influx rate to tumors	0.000173	9.2
k_2 (h^{-1})	efflux rate to tumors	0.0197	fixed[a]
v_1	CPT-induced influx enhancement factor	12.51	11.7
v_2	CPT-induced efflux enhancement factor	3.10	fixed[a]

[a]Efflux parameters were obtained from ref 31.

Tumor Growth Inhibition. The antitumor efficacy of LC-Dox-PoP liposomes irradiated with different DLIs was assessed. As shown in Figure 3A, mice treated with LC-Dox-PoP liposomes with a 1 or 3 h DLI had significantly better tumor regression compared to those treated with a 24 h DLI, when comparing tumor volumes on day 31 ($**p < 0.01$, $*p < 0.05$ respectively). Two out of 6 mice were cured in the 1 h DLI group (33.3% cure rate), and 1 out of 6 mice was cured in the 3 h DLI group (16.7% cure rate). Tumor volumes were not statistically significant different between 1 and 3 h DLI on day 31 ($p > 0.05$). Mice treated with a 1 h DLI had delayed tumor growth for a significantly longer period than those treated with a 6 or 24 h DLI ($*p < 0.05$, $**p < 0.01$ respectively). Mice treated with a 3 h DLI had better tumor growth inhibition than the 24 h DLI group ($*p < 0.05$). The time for tumor volume doubling was faster with longer DLIs (Figure 3B), which is in accordance with the Dox accumulation trend in Figure 2, suggesting that the enhanced efficacy at shorter DLIs is related to the higher drug accumulation in the tumors. The impact of

DOI: 10.1021/acs.molpharmaceut.8b00052
Mol. Pharmaceutics XXXX, XXX, XXX−XXX

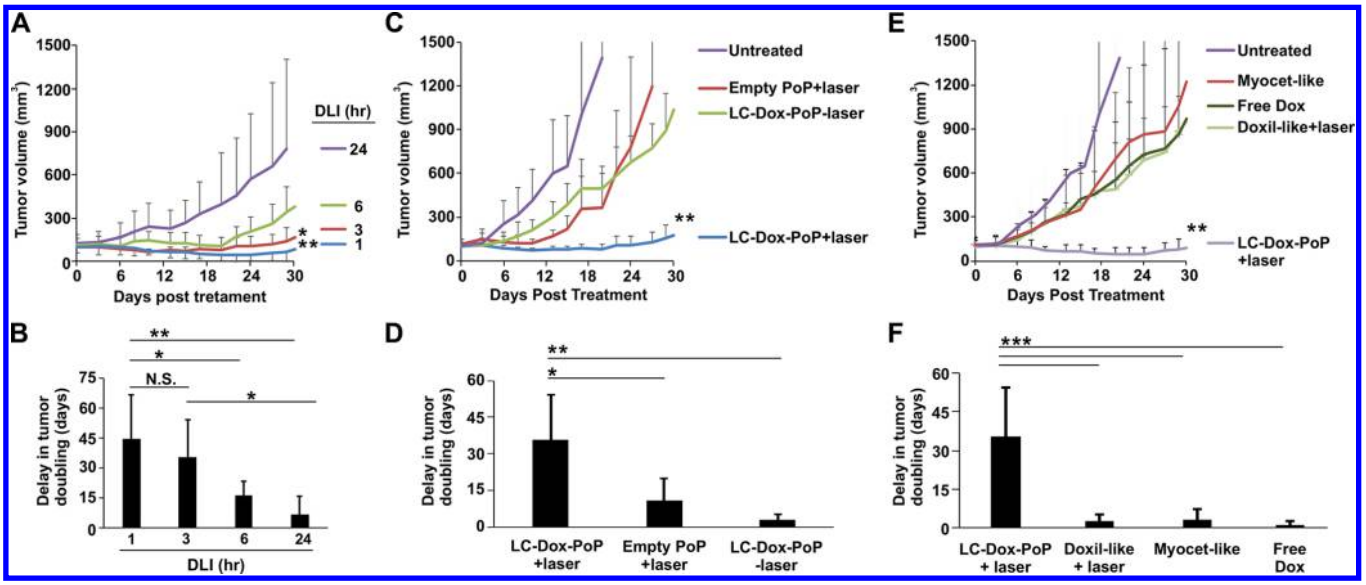

Figure 3. Antitumor efficacy of LC-Dox-PoP liposomes. (A) MIA Paca-2 tumor growth in mice treated with LC-Dox-PoP liposomes and a DLI of 1, 3, 6, or 24 h. Asterisks indicate significant differences in the day 29 tumor volume compared to the 24 h DLI group. (B) Tumor volume doubling delay. (C) Tumor growth after treatment with LC-Dox-PoP liposomes treated with laser (3 h DLI), empty PoP liposomes + laser (1 h DLI), LC-Dox-PoP liposomes without laser, or untreated control. Asterisks indicate significance differences in the day 29 tumor volume compared to the untreated control group. (D) Tumor volume doubling delay. (E) Tumor growth after treatment with LC-Dox-PoP liposomes + laser (1 h DLI), Doxil-like liposomes + laser (3 h DLI), free doxorubicin, Myocet-like liposomes, or untreated control. All groups except the control group received 2 mg/kg Dox. Asterisks indicate significant differences in the day 29 tumor volume compared to the untreated control group. (F) Tumor volume doubling delay. Data show mean ± SD for $n = 6$ mice per group. Statistical tests were performed with one-way ANOVA followed by post hoc Tukey's test: $*p < 0.5$; $**p < 0.01$; $***p < 0.001$; N.S., not significant.

vascular PDT effects at different DLIs still needs to be further studied.

Tumor-bearing mice that received LC-Dox-PoP liposomes with laser treatment had significant tumor growth inhibition compared to the untreated control group (Figure 3C). The efficacy of LC-Dox-PoP liposomes with laser treatment is a combination of chemotherapy and PDT effect. Chemotherapy with LC-Dox-PoP liposomes alone without laser treatment was able to delay the tumor doubling times by 3 (±2) days, while PDT with empty PoP liposomes with laser treatment delayed the tumor doubling time by 11 (±9) days (Figure 3D). LC-Dox-PoP liposomes with laser treatment (3 h DLI) delayed the tumor volume doubling for a significantly longer period (36 ± 19 days) compared to no laser treatment (Figure 3D, $**p < 0.01$, 3 ± 2 days) and empty PoP + laser groups ($*p < 0.01$, 11 ± 9 days). The combined delay in tumor volume doubling induced by chemotherapy alone and photodynamic therapy alone (14 days) was smaller than that induced by CPT (36 days), suggesting a synergistic effect between the chemotherapy and PDT contributions of CPT, in accordance with our previous findings.[2,40]

Doxil, Myocet, and free Dox are three alternative formulations of Dox that are clinically available for chemotherapy. Doxil and Myocet are liposomes, and we generated formulations similar in composition to these. Mice were treated with these Dox formulations at a dose of 2 mg/kg Dox. Only in mice that received LC-Dox-PoP liposomes with laser treatment were tumor volumes significantly smaller than in the untreated control group ($**p < 0.01$, Figure 3E). The other three Dox formulations had minimal impact on tumor growth delay, and there was not a significant difference with the untreated group ($p > 0.05$). There was no significant difference between Doxil-like with laser treatment, Myocet-like, and free Dox groups. Doxil-like with laser treatment, Myocet-like, or free Dox at 2 mg/kg Dox only delayed tumor volume doubling for 2−4 days, whereas LC-Dox-PoP liposomes with laser treatment (3 h DLI) delayed the tumor doubling time for over 35 days (Figure 3F). LC-Dox-PoP liposomes with laser treatment inhibited the tumor growth for a longer period than Doxil-like + laser treatment (3 h DLI), Myocet-like, and free Dox ($***p < 0.001$, $***p < 0.001$, $***p < 0.001$ respectively). Altogether, at 2 mg/kg Dox, LC-Dox-PoP liposomes with CPT clearly induced tumor regression and inhibited tumor growth, whereas Doxil-like liposomes with laser treatment, Myocet-like liposomes, or free Dox had minimal efficacy.

Toxicity. To assess the potential toxicity of LC-Dox-PoP liposomes, mice were treated with 2 mg/kg LC-Dox-PoP liposomes. The absolute Dox concentration in organs after administration of 2 mg/kg LC-Dox-PoP liposomes was relatively low, suggesting low toxicity to key organs (Figure S1A). Mice remained healthy over a two-week period after intravenous dosing with 2 mg/kg LC-Dox-PoP liposomes, as demonstrated by a lack of weight loss or behavior changes (Figure S1B). At the two-week time point, mice were euthanized and blood tests were carried out and compared to untreated mice. Liver function tests indicated that hepatic function of the mice was normal, with no obvious change in bile acids and alanine transferase (Figure 4A). There was some increase of calcium ($*p < 0.05$). There was some increase in creatinine, however, it is still in the typical range, indicating that the kidney function was normal. A complete blood count test indicated that there was some minor increase of white blood cells (WBC, $*p < 0.05$), lymphocytes (LYM, $*p < 0.05$), and neutrophils (NEU,$*p < 0.05$), implying that LC-Dox-PoP liposomes at a low dose of 2 mg/kg can stimulate immune responses (Figure 4B). Altogether, no obvious toxicity was found for LC-Dox-PoP liposomes at 2 mg/kg, and some mild immune stimulatory effects were observed. Potential cytotox-

DOI: 10.1021/acs.molpharmaceut.8b00052
Mol. Pharmaceutics XXXX, XXX, XXX−XXX

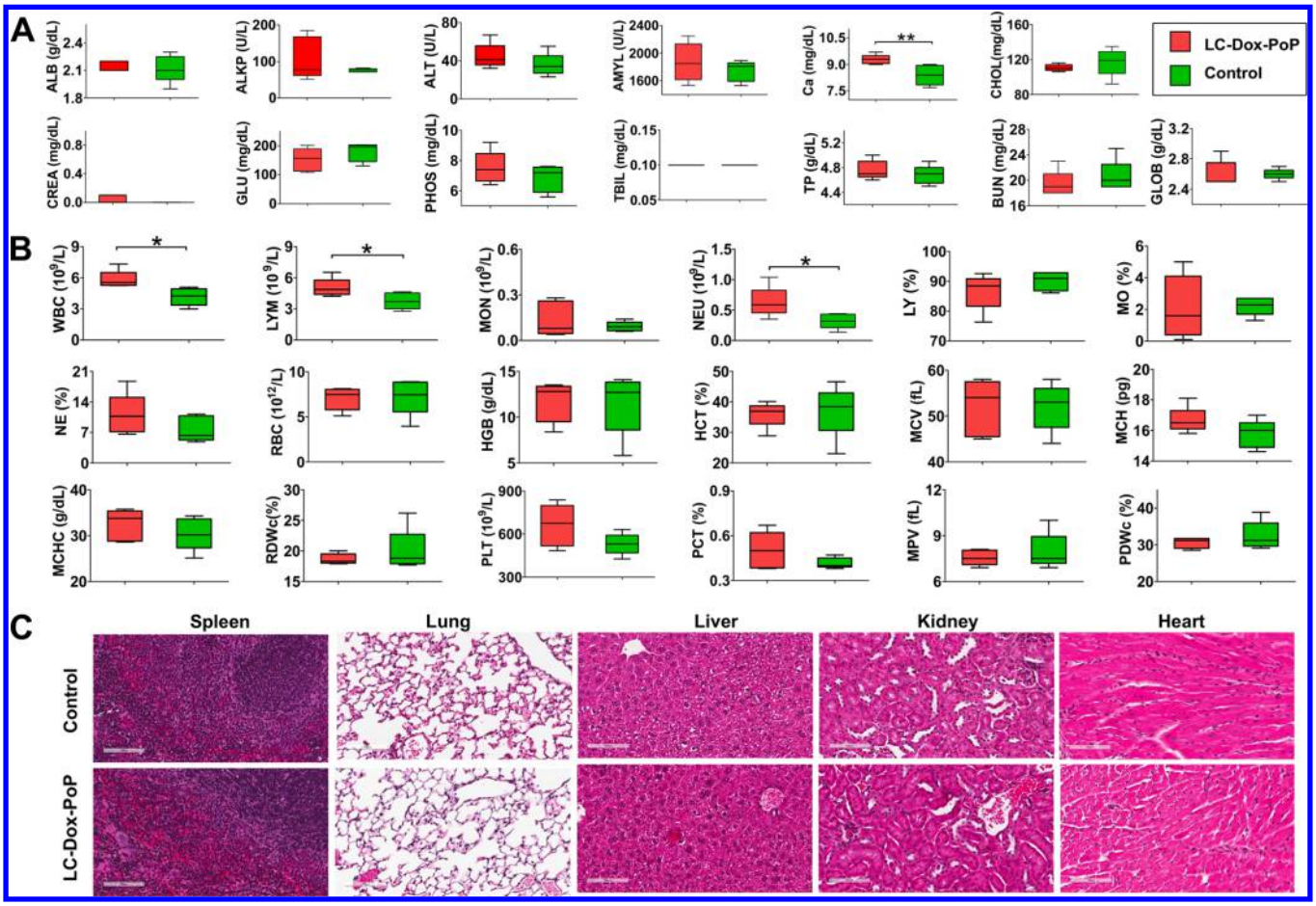

Figure 4. Toxicity after single dose administration of 2 mg/kg LC-Dox-PoP liposomes. (A) Serum chemistry profile and (B) complete blood count of treated and control mice 2 weeks after treatment. Data show box-and-whiskers plot for $n = 5$ mice per group. Statistically different groups based on a two tailed t test are indicated with asterisks. (C) H&E staining of key organs. Scale bars of 100 μm are shown.

icity to key organs was examined by H&E staining. No obvious cytotoxicity was found to the heart, kidney, liver, lung, and spleen after intravenous administration of 2 mg/kg LC-Dox-PoP liposomes (Figure 4C).

CONCLUSION

In mice, LC-Dox-PoP at a 2 mg/kg intravenous Dox dose provided for comparable serum concentrations and pharmacokinetics of Dox as human clinical dosing with 50 mg/m^2 DOXIL. This enables the mimicking of the photosensitizer and Dox concentrations (and thus photo-vascular phenomena) that are anticipated to be encountered in translation of this approach to human studies. At a dose of 2 mg/kg, which is low for murine studies involving Dox, LC-Dox-PoP liposomes substantially (12.5-fold increase of tumor influx rate) increased tumoral drug accumulation. Shorter drug–light intervals led to greater tumoral drug accumulation. Improved antitumor efficacy was also observed for LC-Dox-PoP liposomes when treated at short DLIs. CPT with LC-Dox-PoP liposomes induced tumor regression and growth inhibition, whereas alternative Dox formulations for chemotherapy had minimal efficacy when applied at the same dose. Preliminary toxicity studies did not reveal any LC-Dox-PoP toxicity at the functional dose. Together, these data show that CPT with LC-Dox-PoP at physiologically relevant concentrations is an effective tumor treatment modality, and short drug–light intervals may be preferable. These studies were based on a single xenograft murine tumor model (MIA PaCa-2), so additional testing in other and larger tumor models is warranted.

ASSOCIATED CONTENT

Supporting Information

The Supporting Information is available free of charge on the ACS Publications website at DOI: 10.1021/acs.molpharmaceut.8b00052.

Biodistribution and mouse weight following treatment with LC-Dox-PoP (PDF)

AUTHOR INFORMATION

Corresponding Author

*E-mail: jflovell@buffalo.edu.

ORCID

Jonathan F. Lovell: 0000-0002-9052-884X

Notes

The authors declare no competing financial interest.

ACKNOWLEDGMENTS

This work was supported by the National Institutes of Health (R01EB017270, DP5OD017898) and the National Science Foundation (1555220). This research was supported in part by a Graduate Student Fellowship Award from the American Association of Pharmaceutical Scientists Foundation.

DOI: 10.1021/acs.molpharmaceut.8b00052
Mol. Pharmaceutics XXXX, XXX, XXX–XXX

REFERENCES

(1) Zuluaga, M. F.; Lange, N. Combination of photodynamic therapy with anti-cancer agents. *Curr. Med. Chem.* **2008**, *15* (17), 1655−73.

(2) Luo, D.; Carter, K. A.; Miranda, D.; Lovell, J. F. Chemophototherapy: An Emerging Treatment Option for Solid Tumors. *Adv. Sci.* **2017**, *4* (1), 1600106.

(3) Zhan, C.; Wang, W.; McAlvin, J. B.; Guo, S.; Timko, B. P.; Santamaria, C.; Kohane, D. S. Phototriggered Local Anesthesia. *Nano Lett.* **2016**, *16* (1), 177−181.

(4) Rwei, A. Y.; Wang, W.; Kohane, D. S. Photoresponsive nanoparticles for drug delivery. *Nano Today* **2015**, *10* (4), 451−467.

(5) Rwei, A. Y.; Lee, J.-J.; Zhan, C.; Liu, Q.; Ok, M. T.; Shankarappa, S. A.; Langer, R.; Kohane, D. S. Repeatable and adjustable on-demand sciatic nerve block with phototriggerable liposomes. *Proc. Natl. Acad. Sci. U. S. A.* **2015**, *112* (51), 15719−15724.

(6) Timko, B. P.; Dvir, T.; Kohane, D. S. Remotely Triggerable Drug Delivery Systems. *Adv. Mater.* **2010**, *22* (44), 4925−4943.

(7) Spring, B. Q.; Sears, R. B.; Zheng, L. Z.; Mai, Z.; Watanabe, R.; Sherwood, M. E.; Schoenfeld, D. A.; Pogue, B. W.; Pereira, S. P.; Villa, E.; Hasan, T. A photoactivable multi-inhibitor nanoliposome for tumour control and simultaneous inhibition of treatment escape pathways. *Nat. Nanotechnol.* **2016**, *11* (4), 378−387.

(8) You, J.; Zhang, P.; Hu, F.; Du, Y.; Yuan, H.; Zhu, J.; Wang, Z.; Zhou, J.; Li, C. Near-Infrared Light-Sensitive Liposomes for the Enhanced Photothermal Tumor Treatment by the Combination with Chemotherapy. *Pharm. Res.* **2014**, *31* (3), 554−565.

(9) You, J.; Zhang, G.; Li, C. Exceptionally High Payload of Doxorubicin in Hollow Gold Nanospheres for Near-Infrared Light-Triggered Drug Release. *ACS Nano* **2010**, *4* (2), 1033−1041.

(10) Fomina, N.; Sankaranarayanan, J.; Almutairi, A. Photochemical mechanisms of light-triggered release from nanocarriers. *Adv. Drug Delivery Rev.* **2012**, *64* (11), 1005−1020.

(11) Miranda, D.; Carter, K.; Luo, D.; Shao, S.; Geng, J.; Li, C.; Chitgupi, U.; Turowski, S. G.; Li, N.; Atilla-Gokcumen, G. E.; Spernyak, J. A.; Lovell, J. F. Multifunctional Liposomes for Image-Guided Intratumoral Chemo-Phototherapy. *Adv. Healthcare Mater.* **2017**, *6* (16), 1700253.

(12) Carter, K. A.; Luo, D.; Razi, A.; Geng, J.; Shao, S.; Ortega, J.; Lovell, J. F. Sphingomyelin Liposomes Containing Porphyrin-phospholipid for Irinotecan Chemophototherapy. *Theranostics* **2016**, *6* (13), 2329−2336.

(13) Carter, K. A.; Wang, S.; Geng, J.; Luo, D.; Shao, S.; Lovell, J. F. Metal Chelation Modulates Phototherapeutic Properties of Mitoxantrone-Loaded Porphyrin-Phospholipid Liposomes. *Mol. Pharmaceutics* **2016**, *13* (2), 420−7.

(14) Carter, K. A.; Shao, S.; Hoopes, M. I.; Luo, D.; Ahsan, B.; Grigoryants, V. M.; Song, W.; Huang, H.; Zhang, G.; Pandey, R. K.; Geng, J.; Pfeifer, B. A.; Scholes, C. P.; Ortega, J.; Karttunen, M.; Lovell, J. F. Porphyrin-phospholipid liposomes permeabilized by near-infrared light. *Nat. Commun.* **2014**, *5*, 3546.

(15) Luo, D.; Goel, S.; Liu, H.-J.; Carter, K. A.; Jiang, D.; Geng, J.; Kutyreff, C. J.; Engle, J. W.; Huang, W.-C.; Shao, S.; Fang, C.; Cai, W.; Lovell, J. F. Intrabilayer 64Cu Labeling of Photoactivatable, Doxorubicin-Loaded Stealth Liposomes. *ACS Nano* **2017**, *11* (12), 12482−12491.

(16) Chitgupi, U.; Shao, S.; Carter, K. A.; Huang, W.-C.; Lovell, J. F. Multicolor Liposome Mixtures for Selective and Selectable Cargo Release. *Nano Lett.* **2018**, *18* (2), 1331−1336.

(17) Luo, D.; Carter, K. A.; Razi, A.; Geng, J.; Shao, S.; Giraldo, D.; Sunar, U.; Ortega, J.; Lovell, J. F. Doxorubicin encapsulated in stealth liposomes conferred with light-triggered drug release. *Biomaterials* **2016**, *75*, 193−202.

(18) Luo, D.; Carter, K. A.; Razi, A.; Geng, J.; Shao, S.; Lin, C.; Ortega, J.; Lovell, J. F. Porphyrin-phospholipid liposomes with tunable leakiness. *J. Controlled Release* **2015**, *220* (Part A), 484−494.

(19) Chen, B.; Pogue, B. W.; Luna, J. M.; Hardman, R. L.; Hoopes, P. J.; Hasan, T. Tumor vascular permeabilization by vascular-targeting photosensitization: effects, mechanism, and therapeutic implications. *Clin. Cancer Res.* **2006**, *12* (3 Part 1), 917−923.

(20) Snyder, J. W.; Greco, W. R.; Bellnier, D. A.; Vaughan, L.; Henderson, B. W. Photodynamic therapy: a means to enhanced drug delivery to tumors. *Cancer Res.* **2003**, *63* (23), 8126−8131.

(21) Sano, K.; Nakajima, T.; Choyke, P. L.; Kobayashi, H. Markedly enhanced permeability and retention effects induced by photoimmunotherapy of tumors. *ACS Nano* **2013**, *7* (1), 717−24.

(22) Zhen, Z.; Tang, W.; Chuang, Y.-J.; Todd, T.; Zhang, W.; Lin, X.; Niu, G.; Liu, G.; Wang, L.; Pan, Z.; Chen, X.; Xie, J. Tumor Vasculature Targeted Photodynamic Therapy for Enhanced Delivery of Nanoparticles. *ACS Nano* **2014**, *8* (6), 6004−6013.

(23) Triesscheijn, M.; Ruevekamp, M.; Aalders, M.; Baas, P.; Stewart, F. A. Outcome of mTHPC mediated photodynamic therapy is primarily determined by the vascular response. *Photochem. Photobiol.* **2005**, *81* (5), 1161−7.

(24) Veenhuizen, R.; Oppelaar, H.; Ruevekamp, M.; Schellens, J.; Dalesio, O.; Stewart, F. Does tumour uptake of Foscan determine PDT efficacy? *Int. J. Cancer* **1997**, *73* (2), 236−9.

(25) Dougherty, T. J.; Kaufman, J. E.; Goldfarb, A.; Weishaupt, K. R.; Boyle, D.; Mittleman, A. Photoradiation Therapy for the Treatment of Malignant Tumors. *Cancer Res.* **1978**, *38* (8), 2628−2635.

(26) Cramers, P.; Ruevekamp, M.; Oppelaar, H.; Dalesio, O.; Baas, P.; Stewart, F. A. Foscan uptake and tissue distribution in relation to photodynamic efficacy. *Br. J. Cancer* **2003**, *88* (2), 283−90.

(27) Chen, B.; de Witte, P. A. Photodynamic therapy efficacy and tissue distribution of hypericin in a mouse P388 lymphoma tumor model. *Cancer Lett.* **2000**, *150* (1), 111−7.

(28) Gomer, C. J.; Ferrario, A. Tissue distribution and photosensitizing properties of mono-L-aspartyl chlorin e6 in a mouse tumor model. *Cancer Res.* **1990**, *50* (13), 3985−3990.

(29) Luo, D.; Li, N.; Carter, K. A.; Lin, C.; Geng, J.; Shao, S.; Huang, W. C.; Qin, Y.; Atilla-Gokcumen, G. E.; Lovell, J. F. Rapid Light-Triggered Drug Release in Liposomes Containing Small Amounts of Unsaturated and Porphyrin-Phospholipids. *Small* **2016**, *12* (22), 3039−47.

(30) Bulbake, U.; Doppalapudi, S.; Kommineni, N.; Khan, W. Liposomal Formulations in Clinical Use: An Updated Review. *Pharmaceutics* **2017**, *9* (2), 12.

(31) Luo, D.; Carter, K.; Moline, E. A. G.; Straubinger, N. L.; Geng, J.; Shao, S.; Jusko, W. J.; Straubinger, R. M.; Lovell, J. F. Pharmacokinetics and Pharmacodynamics of Liposomal Chemophototherapy in a Pancreatic Tumor Model. Submitted.

(32) Arnold, R. D.; Mager, D. E.; Slack, J. E.; Straubinger, R. M. Effect of repetitive administration of Doxorubicin-containing liposomes on plasma pharmacokinetics and drug biodistribution in a rat brain tumor model. *Clin. Cancer Res.* **2005**, *11* (24 Part 1), 8856−8865.

(33) D'Argenio, D. Z.; Schumitzky, A.; Wang, X. *ADAPT 5 User's Guide: Pharmacokinetic/Pharmacodynamic Systems Analysis Software*; Biomedical Simulations Resource: Los Angeles, 2009.

(34) Gordon, A. N.; Fleagle, J. T.; Guthrie, D.; Parkin, D. E.; Gore, M. E.; Lacave, A. J. Recurrent Epithelial Ovarian Carcinoma: A Randomized Phase III Study of Pegylated Liposomal Doxorubicin Versus Topotecan. *J. Clin. Oncol.* **2001**, *19* (14), 3312−3322.

(35) O'Brien, M. E.; Wigler, N.; Inbar, M.; Rosso, R.; Grischke, E.; Santoro, A.; Catane, R.; Kieback, D. G.; Tomczak, P.; Ackland, S. P.; Orlandi, F.; Mellars, L.; Alland, L.; Tendler, C. Reduced cardiotoxicity and comparable efficacy in a phase III trial of pegylated liposomal doxorubicin HCl (CAELYX™/Doxil®) versus conventional doxorubicin for first-line treatment of metastatic breast cancer. *Ann. Oncol.* **2004**, *15* (3), 440−449.

(36) Nair, A. B.; Jacob, S. A simple practice guide for dose conversion between animals and human. *J. Basic Clini. Pharm.* **2016**, *7* (2), 27−31.

(37) Gabizon, A.; Shmeeda, H.; Barenholz, Y. Pharmacokinetics of pegylated liposomal Doxorubicin: review of animal and human studies. *Clin. Pharmacokinet.* **2003**, *42* (5), 419−36.

(38) Gabizon, A.; Catane, R.; Uziely, B.; Kaufman, B.; Safra, T.; Cohen, R.; Martin, F.; Huang, A.; Barenholz, Y. Prolonged circulation time and enhanced accumulation in malignant exudates of doxorubicin

DOI: 10.1021/acs.molpharmaceut.8b00052
Mol. Pharmaceutics XXXX, XXX, XXX−XXX

encapsulated in polyethylene-glycol coated liposomes. *Cancer Res.* **1994**, *54* (4), 987−992.
(39) Gabizon, A.; Tzemach, D.; Mak, L.; Bronstein, M.; Horowitz, A. T. Dose dependency of pharmacokinetics and therapeutic efficacy of pegylated liposomal doxorubicin (DOXIL) in murine models. *J. Drug Target.* **2002**, *10* (7), 539−48.
(40) Luo, D.; Geng, J.; Li, N.; Carter, K. A.; Shao, S.; Atilla-Gokcumen, G. E.; Lovell, J. F. Vessel-Targeted Chemophototherapy with Cationic Porphyrin-Phospholipid Liposomes. *Mol. Cancer Ther.* **2017**, *16* (11), 2452−2461.

DOI: 10.1021/acs.molpharmaceut.8b00052
Mol. Pharmaceutics XXXX, XXX, XXX−XXX